JACS
JOURNAL OF THE AMERICAN CHEMICAL SOCIETY

Communication

pubs.acs.org/JACS

Microfluidic Assembly of Monodisperse Vesosomes as Artificial Cell Models

Nan-Nan Deng, Maaruthy Yelleswarapu, Lifei Zheng, and Wilhelm T. S. Huck*

Institute for Molecules and Materials, Radboud University, Heyendaalseweg 135, 6525 AJ Nijmegen, The Netherlands

Supporting Information

ABSTRACT: Vesosomes are nested liposomal structures with high potential as advanced drug delivery vehicles, bioreactors and artificial cells. However, to date no method has been reported to prepare monodisperse vesosomes of controlled size. Here we report on a multistep microfluidic strategy for hierarchically assembling uniform vesosomes from dewetting of double emulsion templates. The control afforded by our method is illustrated by the formation of concentric, pericentric and multicompartment liposomes. The microfluidic route to vesosomes offers an exceptional platform to build artificial cells as exemplified by the in vitro transcription in "nucleus" liposomes and the mimicry of the architecture of eukaryotic cells. Finally, we show the transport of small molecules across the nucleic envelope via insertion of nanopores into the bilayers.

Vesosomes are multicompartmental liposomal structures of varied architectures.[1] These multivesicular vesicles can consist of multilayered concentric liposomes, or multiple liposomes arranged within or around large liposomes. These structures, as well as related multicompartment polymersomes[2] and proteinosomes,[3] have generated significant interest for their potential as drug delivery vehicles,[1a,4] compartmentalized nano- or microscale bioreactors,[5] or as artificial cell/protocell models.[6] Zasadzinski and co-workers have shown that vesosomes can protect encapsulated drug carrying compartments from blood components due to the presence of double bilayers,[4b] and slow the release of vesicle contents.[4c] Bolinger et al.[5b,c] employed multicompartment vesosomes to perform consecutive enzymatic reactions by thermally remote release of different compounds encapsulated in smaller liposomes. Remarkably, vesosomes that contain a "nucleus" or "organelles" represent a new concept toward the design of artificial cells, especially artificial eukaryotic cells.[6a] However, conventional methods,[7] such as bulk hydration[8] or electroformation[9] of dried lipid membranes, do not readily yield complex hierarchical vesicular structures, and certainly do not provide any control over dimensions, offer low encapsulation efficiencies and low yields. Moreover, these strategies do not allow a systematic simultaneous loading of different components into diverse compartments. These limitations have severely hindered progress in the application of such multivesicular liposomes. Recently, droplet microfluidics has been shown to offer excellent emulsion templates for the preparation of monodisperse liposomes[10] as well as polymersomes,[2,11] but no vesosomes have been reported.

Recently, we have presented a surfactant-assisted microfluidic strategy for assembling monodisperse liposomes from water-in-oil-in-water (W/O/W) double emulsion droplets.[10a] In this paper, we demonstrate the hierarchical assembly of uniform vesosomes via multidewetting processes. Briefly, the single liposomes formed from dewetting of microfluidically prepared W/O/W emulsion droplets were reinjected into microfluidic devices as the inner phase to fabricate larger liposome-loaded W/O/W emulsion droplets, which will undergo a second dewetting transition to form uniform liposome-in-liposome vesicles. The control afforded by our method is illustrated by the formation of concentric, pericentric and multicompartment liposomes. Finally, we show the resultant vesosomes are potentially used as complex artificial cell models.

To produce monodisperse vesosomes, we first fabricated monodisperse single liposomes as the "nuclei" according to our recent publication (Figure S1).[10a] Subsequently, the preformed single liposomes dispersed in an aqueous phase (W1, see SI Materials for details) were reinjected into the microfluidic device as inner phase to make larger W/O/W double emulsion droplets (Figures 1a, b1, S2 and Movies S1 and S2, see SI Materials for details of the middle oil phase (O) and the outer water phase (W2)). In this way, smaller liposomes were successfully loaded into the inner droplets of double emulsions. As we reported previously,[10a] the dewetting transition is induced by the spontaneous reduction of the interfacial energies of the W1/O/W2 emulsion system, i.e., a positive spreading coefficient of phase W2. Along with the evaporation of chloroform in the oil phase, the oil shells of the larger double emulsion droplets gradually dewet from the interior drops (Figures 1b2 and S3), forming vesosomes and separated oil drops containing excess lipids (Figures 1b3 and S3). To visualize the vesosomes clearly, fluorescein isothiocyanate-dextran (FITC-Dextran) and rhodamine B isothiocyanate-Dextran (RITC-dextran) were respectively used to label the inner and outer liposomes (Figures 1c,d,f and S3). As Figure 1c shows, the resultant vesosomes are uniform; their internal and external mean diameters are 43 and 102 μm respectively and their coefficients of variation are 5% and 3% respectively (Figure 1e). Notably, the yield of vesosomes with single inner liposomes is as high as 66.4% (Figures S4 and S5).

This microfluidic method gives control over the vesosome dimensions and configurations. The number of the interior liposomes can be varied by tuning the flow rate. For example, we fixed the flow rates of middle and outer phases at 300 and

Received: October 20, 2016
Published: December 15, 2016

DOI: 10.1021/jacs.6b10977
J. Am. Chem. Soc. 2017, 139, 587−590

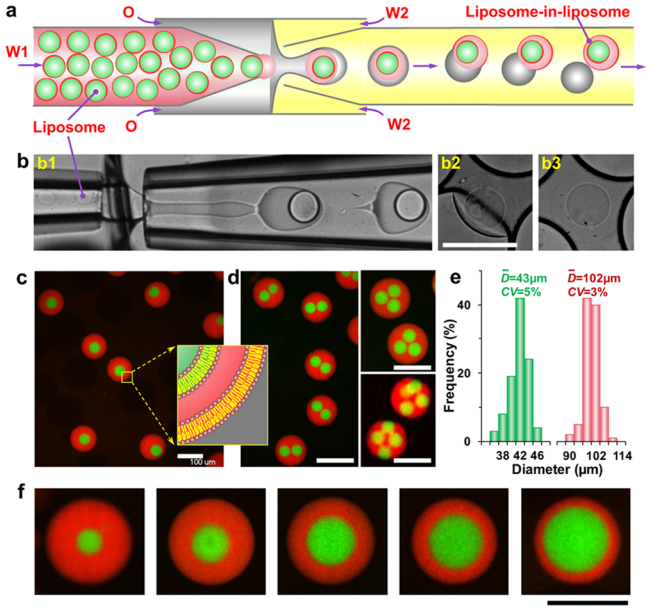

Figure 1. (a,b) Schematics and snapshots of the microfluidic preparation of double emulsions with an inner liposome and the assembly of vesosomes from emulsion dewetting. (c,d) Confocal images of the monodisperse vesosomes with one, two, three and four inner liposomes. (e) Size distribution of inner and outer liposomes of the vesosomes in panel c. (f) As-formed vesosomes with different-sized interior liposomes. Scale bars, 100 μm.

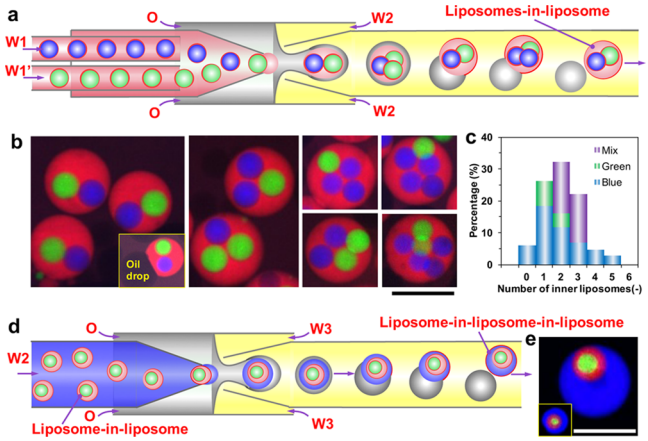

Figure 2. (a) Schematics of the microfluidic preparation of double emulsions with distinct interior liposomes and the dewetting process. (b) Confocal images of the vesosomes with different numbers and ratios of interior liposomes. Inset in panel b is an emulsion template undergoing dewetting. (c) Distribution of the number of inner liposomes of as-formed vesosomes (Figure S13, N = 329). (d,e) Formation of triple vesosomes and the resultant structures. Scale bars, 100 μm.

2500 μL h^{-1}, and adjusted the inner phase flow rates from 150, 280 to 360 μL h^{-1} to prepare vesosomes that mainly contain one and two to four inner liposomes (Figure 1c,d). The distribution of numbers of encapsulated liposomes shows an overall growing trend (Figures S4–S9), and the yields of each main products are more than 20%. Besides, by slowing down the flow rate in outer phase, we also prepared vesosomes that encapsulate 3 to 5 inner liposomes (Figures S10 and S11). In addition, vesosomes with diverse dimensions of subcompartments were also fabricated. As Figures 1f and S12 show, the shell volumes between interior and exterior liposomes can be adjusted, which allow the precise load of ingredients.

Further, the droplet microfluidic technique has shown considerable flexibility in encapsulation of distinct droplets in multiple emulsion droplets,[12] which offers perfect templates to create structured vesosomes. To demonstrate this idea, we upgraded the microfluidic device with two independent inlets (Figure 2a),[10a] which were employed to prepare double emulsion droplets with different liposomes. Similarly, these emulsion templates undergo a complete dewetting to generate vesosomes containing distinct liposomes. As Figure 2b shows, vesosomes with diverse inner structures were successfully achieved. More than 300 vesosomes were collected and analyzed, showing that 32% and 22% of the vesosomes contain 2 and 3 inner liposomes respectively; the rest are empty, or contain one or more than 4 inner liposomes (Figures 2c and S13). We note that the pairing of reinjected liposomes is a key point to generate vesosomes with controlled numbers and types of inner liposomes. The method can be extended to make more complex concentric multicompartment vesosomes, for example, liposome-in-liposome-in-liposome vesosomes (Figure 2d,e).

The vesosomes essentially represent liposomes which contain a "nucleus" or "organelles", and represent a promising new concept toward building artificial cells, especially the artificial eukaryotic cells. Although liposomes have been widely employed as artificial cells to imitate the architectures and functions of prokaryotic cells, such as cell division,[13] RNA replication[14] and in vitro transcription/translation (IVTT),[6c] the mimicry of intracellular compartmentalization both in structures and functions remains underexplored, mostly because the high-order vesicles required, are difficult to make. Furthermore, conventional routes to the vesosomes typically do not efficiently coencapsulate different solutions into different subcompartments. Here, we show the advantages of our microfluidic approach in loading diverse complex components and the potential of the resultant vesosomes in building artificial cells.

To mimic the key function of cell nuclei, we encapsulated an in vitro transcription (IVTx) mix in single liposomes to synthesize RNA (Figure 3a). This mix contains T7 RNAP, pyrophosphatase, DNA template, RNase inhibitor and feeding buffer (see SI IVTx in nucleus liposomes and IVTT for details), and all components were successfully loaded in inner droplets during the double emulsion template preparation. To visualize the RNA generation, we coded the plasmids with a sequence for Spinach2 aptamer that can bind a dye called 5-difluoro-4-hydroxybenzylidene imidazolinone (DFHBI) to form a fluorescent complex of Spinach2-DFHBI (Figure 3b); both DFHBI and Spinach2 are nonfluorescent until binding occurs.[15] As Figures 3c,d, S14 and Movie S4 show the fluorescence intensity of Spinach2-DFHBI in liposomes notably increased from 0 to 60 min and up to 120 min during the IVTx. After 2 h expression, the fluorescence signal reached a plateau probably due to running out of nutrients (Figure 3d). This agrees well with the IVTx reaction in bulk recorded by a plate reader (Figure S15).

To mimic the architecture of eukaryotic cells, we embedded the single liposomes that contain IVTx mix as artificial nuclei into larger liposomes. In the larger droplets, IVTT mix (consisting of one-third *Escherichia coli* cell lysate and two-thirds feeding buffer, see SI IVTx in nucleus liposomes and IVTT for details)[16] for monomeric red fluorescent protein

DOI: 10.1021/jacs.6b10977
J. Am. Chem. Soc. 2017, 139, 587–590

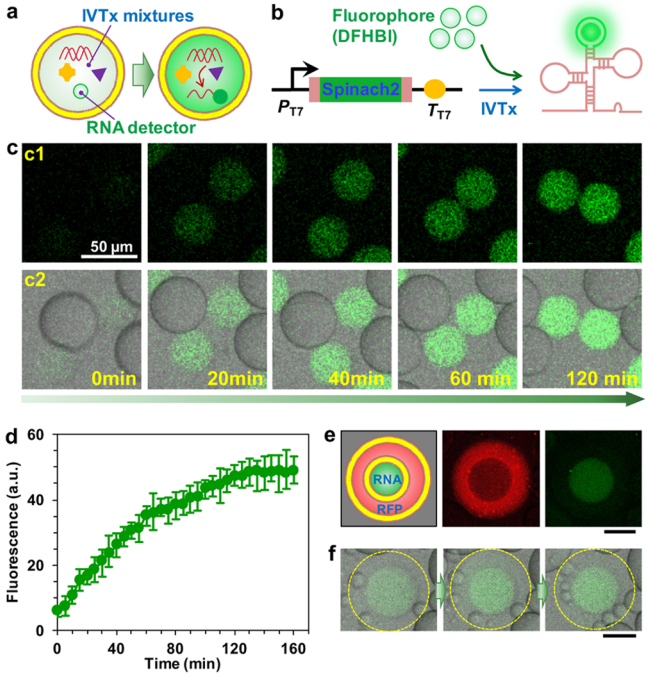

Figure 3. (a,b) Cartoons showing in situ detection of IVTx inside the liposomes (a) and the working principle of the RNA aptamer Spinach2 (b). (c) Sequence of images showing synthesis of RNA in the liposomes. (d) RNA expression kinetics. (e) Independent encapsulation of IVTx mix into interior liposomes and IVTT mix into exterior liposomes. (f) IVTx in nucleus liposome of vesosomes. Scale bars, 50 μm.

(mRFP) was encapsulated to form a kind of "cytoplasm" phase (Figure 3e). RNA was successfully expressed inside the nucleus liposomes as shown in Figures 3e (last image) and 3f. Moreover, most of the artificial cell models are stable for more than 8 h, which is sufficient for IVTT or related research. Recently, we already demonstrated the in vitro expression of enhanced green fluorescent protein in liposomes.[10a] As we here show that transcription and translation can in principle be carried out in two different compartments of the artificial cells, the final key (and probably most challenging) step would be to realize the transfer of RNA across lipid bilayers.

The controlled passage of nutrient molecules and wastes is a key feature of biological cells, in which the nanopores play an important role in both cell envelops and nucleic shells. Therefore, to demonstrate the feasibility of molecule transfer between subcompartments, we inserted a membrane protein melittin into the nucleus liposomes to create nanopores. Melittin self-assembles into bilayers to create pores of 1−3 nm or 3.5−4.5 nm in diameter depending on the number of assembly subunits,[17] which allows small molecules to transfer. As Figure 4a shows, we loaded the inner liposomes with melittin monomers (2 μM) and calcein fluorescent molecules (Mw = 623 g mol^{-1}, 10 μM) and outer liposomes with RITC-Dextran (average Mw = 70000 g mol^{-1}), and then observed the fluorescence intensity over time. Once the nanopores were formed in the nucleus bilayers, the green dye (calcein) in the inner liposomes rapidly (about 2 min) diffused into the outer liposomes, while the red dye (RITC-Dextran) in the outer liposome failed to diffuse into the inside because of the larger molecule weight (Figure 4b, Movie S5). This size exclusion phenomenon also indicates that the morphologies of both the inner and outer liposomes are intact, ensuring that the release of the fluorescent molecules is not because of the burst of inner liposomes. After the dye diffusion, the distribution of calcein in the vesosomes is homogeneous (Figure 4b calcein channel and Figure 4e curves 1 and 2). In contrast, in the absence of membrane proteins, no dye transfer was observed even after 2 h (Figure 4c−e, Movie S3). Furthermore, it has been reported that insertion of other membrane proteins into the bilayers forms nanopores of different sizes, for example, alpha-hemolysin (αHL) creates pores of 1.4 nm in diameter.[18] Therefore, it is feasible to insert selectively different membrane proteins, for example, melittin and αHL, into internal and external liposomes respectively to create different nanopores, which will endow different vesosome compartments with

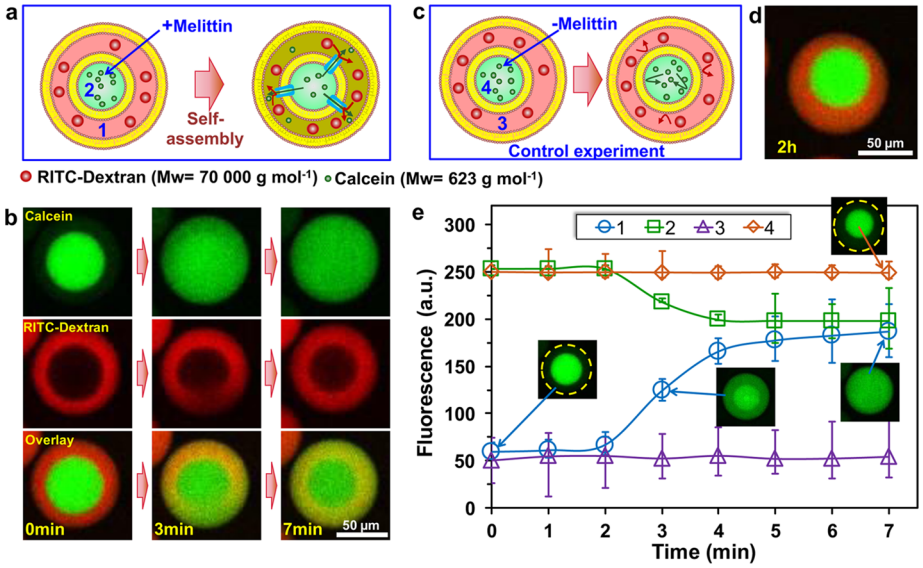

Figure 4. (a) Cartoons and (b) confocal image series show protein pore-mediated transport of fluorescent molecules from inner liposomes to outer liposomes. (c,d) Control experiment: no melittin was added. (e) Kinetics of time-dependent release of calcein from inner liposome to outer liposome. The curves 1, 2, 3 and 4 refer to the fluorescence in relevant liposomes as shown in panels a and c. Scale bars, 50 μm.

DOI: 10.1021/jacs.6b10977
J. Am. Chem. Soc. 2017, 139, 587−590

different permeability properties. This will open up platforms to study the communications between artificial cell compartments and that between compartment and surrounding environment.

In summary, we have reported a multistep microfluidic strategy for the hierarchical assembly of uniform vesosomes from dewetting of W/O/W double emulsion droplets. To show the control over vesosome formation, concentric, pericentric and multicompartment liposomes were successfully created. These structures offer an advanced platform to build artificial cell models as exemplified by the encapsulation of solutions as complex as that for IVTx and IVTT into the different compartments, and real time detection of RNA generation. Finally, we showed the insertion of nanopores into the nucleus liposomes, which allows for the transport of small molecules across the envelopes. Future work will focus on nanopore-mediated transfer of RNA across bilayers and coupled IVTT in vesosome systems. We believe that this approach for fabricating uniform vesosomes with well-defined sizes, will facilitate artificial cell related research like enzyme storage and release, membrane fusion, vesicle transport and multistep bioprocesses.

■ ASSOCIATED CONTENT

Supporting Information

The Supporting Information is available free of charge on the ACS Publications website at DOI: 10.1021/jacs.6b10977.

Experimental section and figures(PDF)

Reinjection of liposomes into the microfluidic device (AVI)

Microfluidic preparation of W/O/W emulsion droplets loaded with single liposomes (AVI)

Microfluidic preparation of W/O/W emulsion droplets loaded with two liposomes (AVI)

In vitro transcription and real-time detection of RNA in liposomes (AVI)

Insertion of nanopores into the bilayers of nucleus liposomes to transport fluorescent molecules (AVI)

■ AUTHOR INFORMATION

Corresponding Author

*w.huck@science.ru.nl

ORCID

Nan-Nan Deng: 0000-0001-7183-7973

Wilhelm T. S. Huck: 0000-0003-4222-5411

Notes

The authors declare no competing financial interest.

■ ACKNOWLEDGMENTS

This work was supported by The Netherlands Organization for Scientific Research (NWO, TOPPUNT grant 718.014.001, the Ministry of Education, Culture and Science (Gravity programme, 024.001.035), and a Marie Skłodowska-Curie Actions Individual Fellowship to N.-N.D. (EC, H2020-MSCA-IF grant 659907). We thank Sandra Wardle (Radboud University) and Laure Eydieux (Polytech Clermont-Ferrand) for their help with the RNA aptamer preparation.

■ REFERENCES

(1) (a) Kisak, E. T.; Coldren, B.; Evans, C. A.; Boyer, C.; Zasadzinski, J. A. *Curr. Med. Chem.* **2004**, *11*, 199−219. (b) Torchilin, V.; Weissig, V. *Liposomes: a practical approach*; Oxford University Press: Oxford; New York, 2003.

(2) (a) Shum, H. C.; Zhao, Y.-j.; Kim, S.-H.; Weitz, D. A. *Angew. Chem., Int. Ed.* **2011**, *50*, 1648−1651. (b) Kim, S.-H.; Shum, H. C.; Kim, J. W.; Cho, J.-C.; Weitz, D. A. *J. Am. Chem. Soc.* **2011**, *133*, 15165−15171.

(3) (a) Liu, X.; Zhou, P.; Huang, Y.; Li, M.; Huang, X.; Mann, S. *Angew. Chem.* **2016**, *128*, 7211−7216. (b) Huang, X.; Patil, A. J.; Li, M.; Mann, S. *J. Am. Chem. Soc.* **2014**, *136*, 9225−9234.

(4) (a) Marguet, M.; Edembe, L.; Lecommandoux, S. *Angew. Chem., Int. Ed.* **2012**, *51*, 1173−1176. (b) Wong, B.; Boyer, C.; Steinbeck, C.; Peters, D.; Schmidt, J.; van Zanten, R.; Chmelka, B.; Zasadzinski, J. A. *Adv. Mater.* **2011**, *23*, 2320−2325. (c) Boyer, C.; Zasadzinski, J. A. *ACS Nano* **2007**, *1*, 176−182.

(5) (a) Peters, R. J. R. W.; Marguet, M.; Marais, S.; Fraaije, M. W.; van Hest, J. C. M.; Lecommandoux, S. *Angew. Chem., Int. Ed.* **2014**, *53*, 146−150. (b) Bolinger, P.-Y.; Stamou, D.; Vogel, H. *Angew. Chem., Int. Ed.* **2008**, *47*, 5544−5549. (c) Bolinger, P.-Y.; Stamou, D.; Vogel, H. *J. Am. Chem. Soc.* **2004**, *126*, 8594−8595.

(6) (a) Marguet, M.; Bonduelle, C.; Lecommandoux, S. *Chem. Soc. Rev.* **2013**, *42*, 512−529. (b) Elani, Y.; Law, R. V.; Ces, O. *Nat. Commun.* **2014**, *5*, 5305. (c) Noireaux, V.; Libchaber, A. *Proc. Natl. Acad. Sci. U. S. A.* **2004**, *101*, 17669−17674. (d) Huang, X.; Li, M.; Green, D. C.; Williams, D. S.; Patil, A. J.; Mann, S. *Nat. Commun.* **2013**, *4*, 2239.

(7) (a) Discher, D. E.; Eisenberg, A. *Science* **2002**, *297*, 967−973. (b) Walde, P.; Cosentino, K.; Engel, H.; Stano, P. *ChemBioChem* **2010**, *11*, 848−865. (c) Walker, S. A.; Kennedy, M. T.; Zasadzinski, J. A. *Nature* **1997**, *387*, 61−64.

(8) Horger, K. S.; Estes, D. J.; Capone, R.; Mayer, M. *J. Am. Chem. Soc.* **2009**, *131*, 1810−1819.

(9) Montes, L. R.; Alonso, A.; Goñi, F. M.; Bagatolli, L. A. *Biophys. J.* **2007**, *93*, 3548−3554.

(10) (a) Deng, N.-N.; Yelleswarapu, M.; Huck, W. T. S. *J. Am. Chem. Soc.* **2016**, *138*, 7584−7591. (b) Deshpande, S.; Caspi, Y.; Meijering, A. E. C.; Dekker, C. *Nat. Commun.* **2016**, *7*, 10447. (c) Shum, H. C.; Lee, D.; Yoon, I.; Kodger, T.; Weitz, D. A. *Langmuir* **2008**, *24*, 7651−7653. (d) Stachowiak, J. C.; Richmond, D. L.; Li, T. H.; Liu, A. P.; Parekh, S. H.; Fletcher, D. A. *Proc. Natl. Acad. Sci. U. S. A.* **2008**, *105*, 4697−4702. (e) Ota, S.; Yoshizawa, S.; Takeuchi, S. *Angew. Chem., Int. Ed.* **2009**, *48*, 6533−6537. (f) Abkarian, M.; Loiseau, E.; Massiera, G. *Soft Matter* **2011**, *7*, 4610−4614. (g) Funakoshi, K.; Suzuki, H.; Takeuchi, S. *J. Am. Chem. Soc.* **2007**, *129*, 12608−12609. (h) Tan, Y.-C.; Hettiarachchi, K.; Siu, M.; Pan, Y.-R.; Lee, A. P. *J. Am. Chem. Soc.* **2006**, *128*, 5656−5658.

(11) (a) Shum, H. C.; Kim, J.-W.; Weitz, D. A. *J. Am. Chem. Soc.* **2008**, *130*, 9543−9549. (b) Thiele, J.; Chokkalingam, V.; Ma, S.; Wilson, D. A.; Huck, W. T. S. *Mater. Horiz.* **2014**, *1*, 96−101.

(12) (a) Deng, N.-N.; Wang, W.; Ju, X.-J.; Xie, R.; Weitz, D. A.; Chu, L.-Y. *Lab Chip* **2013**, *13*, 4047−4052. (b) Wang, W.; Xie, R.; Ju, X.-J.; Luo, T.; Liu, L.; Weitz, D. A.; Chu, L.-Y. *Lab Chip* **2011**, *11*, 1587−1592.

(13) (a) Osawa, M.; Anderson, D. E.; Erickson, H. P. *Science* **2008**, *320*, 792−794. (b) Kurihara, K.; Tamura, M.; Shohda, K.-i.; Toyota, T.; Suzuki, K.; Sugawara, T. *Nat. Chem.* **2011**, *3*, 775−781.

(14) Chen, I. A.; Salehi-Ashtiani, K.; Szostak, J. W. *J. Am. Chem. Soc.* **2005**, *127*, 13213−13219.

(15) Strack, R. L.; Disney, M. D.; Jaffrey, S. R. *Nat. Methods* **2013**, *10*, 1219−1224.

(16) Sokolova, E.; Spruijt, E.; Hansen, M. M. K.; Dubuc, E.; Groen, J.; Chokkalingam, V.; Piruska, A.; Heus, H. A.; Huck, W. T. S. *Proc. Natl. Acad. Sci. U. S. A.* **2013**, *110*, 11692−11697.

(17) Ladokhin, A. S.; Selsted, M. E.; White, S. H. *Biophys. J.* **1997**, *72*, 1762−1766.

(18) Song, L.; Hobaugh, M. R.; Shustak, C.; Cheley, S.; Bayley, H.; Gouaux, J. E. *Science* **1996**, *274*, 1859−1865.

DOI: 10.1021/jacs.6b10977
J. Am. Chem. Soc. 2017, 139, 587−590